Effect of Sampling Rate on Resolution in Comprehensive Two-Dimensional Liquid Chromatography

ARTICLE *in* ANALYTICAL CHEMISTRY · MARCH 1998

Impact Factor: 5.64 · DOI: 10.1021/ac971184b

3 AUTHORS, INCLUDING:

Joe P. Foley
Drexel University
108 PUBLICATIONS **3,267** CITATIONS

Anal. Chem. **1998,** *70,* 1585−1594

Effect of Sampling Rate on Resolution in Comprehensive Two-Dimensional Liquid Chromatography

Robert E. Murphy,*[,†,‡] Mark R. Schure,[§] and Joe P. Foley[‡]

Analytical Research and Theoretical Separation Science Laboratory, Rohm and Haas Company, 727 Norristown Road, Spring House, Pennsylvania 19477, and Department of Chemistry, Villanova University, Villanova, Pennsylvania 19085

In "comprehensive" two-dimensional liquid chromatography, the column effluent from the first separation system (the first dimension) is sequentially sampled by the second dimension separation system. The total analysis time is largely determined by the speed of the second dimension separation system; the most retained component must elute before the least retained component of the next second dimension separation. Optimization of multidimensional separation systems requires that one understand the relationship between system resolution and the number of second dimension samples across a first dimension peak. In this paper, we study the theoretical and experimental aspects of this sampling process. To obtain high two-dimensional resolution, each peak in the first dimension should be sampled at least three times into the second dimension when the sampling is in-phase. If the sampling is maximally out of phase, there should be at least four samples per peak for high-fidelity separation. The sensitivity of the resolution with respect to the sampling phase is discussed in detail and shown to be insignificant when four or greater samples are taken across the first dimension peak width. These results suggest optimal criteria for method development with multidimensional chromatography.

Two-dimensional liquid chromatographic systems (2DLC) have been used for many years to characterize and separate biomolecules, polymers, and other complex mixtures.[1−3] Natural products and polymer samples are extremely complex, containing a large number of components of various composition and size. Two-dimensional liquid chromatography has the peak capacity to separate plant extracts[1] and the selectivity and resolution to separate copolymers[2] by their size and composition. The most common form of two-dimensional separation is heart-cutting, where one discrete zone is collected from the first dimension column and reinjected into the second dimension separation system.[4−7] The resulting data are two individual one-dimensional data sets and are useful for the higher resolution analysis of a single fused peak from the first dimension. In so-called "comprehensive" automated systems, sequential aliquots from the first dimension effluent are sampled by the second dimension separation system.[8] The resulting data is a matrix, usually represented as a contour plot with each chromatographic separation along an axis. This technique is very useful for the higher resolution analysis of multiple fused peaks from the first dimension column and resolved in the second dimension separation system when orthogonal separation systems can be found.

There are many combinations of separation techniques and methods of coupling these techniques currently employed in multidimensional separation systems. Giddings[9] discussed a number of the possible combinations of techniques that can be coupled together to form two-dimensional systems. We will restrict our discussion to only two-dimensional systems here although many of the principles will apply to more than two coupled separation systems. The two-dimensional techniques can be categorized by the number of fractions and amount of eluent sampled into the second dimension (Table 1). We will focus exclusively on the comprehensive mode, with the entire first dimension effluent sampled by the second dimension separation system in this paper.

A host of methods exist for coupling the various separation systems. An eight-port valve with matching sample loops is typically used for the coupling and repetitive sampling of the first dimension separation system when the comprehensive mode of operation is utilized.[8,10] A six-port valve is generally used for the partial sampling of the first dimension separation with repetitive sampling.[11−13] A direct interface is also possible which utilizes

† Analytical Research, Rohm and Haas Co.
‡ Villanova University.
§ Theoretical Separation Science Laboratory, Rohm and Haas Co.

(1) Erni, F.; Frei, R. W. *J. Chromatogr.* **1978**, *149*, 561−569.
(2) Balke, S. T.; Patel, R. D. *J. Polym. Sci., Polym. Lett. Ed.* **1980**, *18*, 453−456.
(3) Majors, R. E. *J. Chromatogr. Sci.* **1980**, *18*, 571−579.
(4) Augenstein, M.; Strickler, M. *Makromol. Chem.* **1990**, 415−428.
(5) Pasch, H.; Brinkmann, C.; Much, H.; Just, U. *J. Chromatogr.* **1992**, *623*, 315−322.
(6) Van Doremaele, G. H. J.; Geerts, F. H. J. M.; Aan de Meulen, L. J.; German, A. L. *Polymer* **1992**, *33*, 1512−1518.
(7) Brinkman, U. A. Th. *J. Chromatogr., A,* **1994**, *665*, 217−231.
(8) Bushey, M. M.; Jorgenson, J. W. *Anal. Chem.* **1990**, 62, 161−167.
(9) Giddings, J. C. *Anal. Chem.* **1984**, *56*, 1258−1270A.
(10) Rose, D. J.; Opiteck, G. J. *Anal. Chem.* **1994**, *66*, 2529−2536.
(11) Holland, L. A.; Jorgenson, J. W. *Anal. Chem.* **1995**, *67*, 3275−3283.
(12) Lemmo, A. V.; Jorgenson, J. W. *J. Chromatogr.* **1993**, *633*, 213−220.
(13) Venema, E.; de Leeuw, P.; Kraak, J. C.; Poppe, H.; Tijssen, R. *J. Chromatogr., A* **1997**, *765*, 135−144.

S0003-2700(97)01184-0 CCC: $15.00
Published on Web 03/13/1998

Table 1. Nomenclature of Two-Dimensional Techniques

no. of fractions sampled into second dimension	amount sampled into second dimension	
	partial	entire
typically <5 (heart cut)	heart cut LC[3−6] or GC[7]	cross-fractionation[2]
typically >5 and repetitive (comprehensive)	LC/LC (6-port valve)[11]	LC/LC (8-port valve)[1,8,19]
	LC/CE[12]	gel electrophoresis/LC[10]
	thermal FFF/GPC[13]	CE/gel electrophoresis[14]
		TLC/TLC[15]
		PAGE/IEF[16]
		GC/GC[17]

continuous sampling into the second dimension[14] and is similar to 2D thin-layer chromatography[15] and 2D gel electrophoresis.[16]

Perhaps the most challenging applications of two-dimensional separation systems are the separation of polymers, polymer blends, copolymers, and large molecules. Polymers may contain thousands of individual monomers with many inherent distributions. The chromatographic determination of the size, composition, sequence, architecture, or end group distribution of a copolymer can be accomplished using chromatographic techniques provided that the separation is based solely on that distribution[18] and is not sensitive to other distributions that may be inherent in the molecular architecture.

The combination of gel permeation chromatography (GPC) and reversed-phase liquid chromatography (RPLC) in an automated heart-cut system for the simultaneous analysis of the size and composition of copolymers was first reported by Balke[2] (also called polymer cross-fractionation). This mode of operation is quite desirable in polymer characterization and is typically performed off-line with a fraction collector and autosampler. However, speed, higher resolution, and convenience have been driving forces toward performing this type of analysis in the comprehensive mode of operation. For example, Kilz and coworkers have utilized a comprehensive 2DLC (RPLC/GPC) system for the composition and size analysis of copolymers using conventional columns in the first and second dimensions resulting in ≈10-h total run times.[19]

The total analysis time is the product of the second dimension separation system analysis time and the total number of fractions injected into the second dimension. Thus, the analysis time of the second dimension separation system is a major factor in determining the total analysis time of comprehensive two-dimensional separation systems. In 2DLC with RPLC as the first dimension separator and GPC as the second dimension separator, the GPC run time can be significantly reduced without a loss of resolution by using short and smaller particle size columns.[20] Smaller sampling times across the first dimension peak width can aid in decreasing the total analysis time as long as the second dimension resolution is not impaired.

There appears to be little if any information in the literature governing the number of samples per first dimension peak width needed for optimal two-dimensional resolution and speed in comprehensive 2DLC. The optimization of 2DLC resolution and speed, as a function of system variables, will reduce two-dimensional method development time and make the technique more widely used for the characterization of polymers and other difficult separation problems.

In this paper, we investigate the effect of sampling time on two-dimensional resolution by utilizing 2DLC (RPLC/GPC) for the separation of poly(ethylene glycol)s and surfactants with different alkyl and ethylene oxide chain lengths. The sampling time into the second dimension is varied by changing the split ratio of the first dimension column effluent while keeping the sample loop volume and column flow rate constant. The resolution is compared for several sampling times. The results are contrasted with theoretical calculations of zone broadening as a function of sampling time and sampling phase. Zone broadening theory and experiment are shown to be in agreement, and quantitative statements regarding the sampling process are given as operational aids toward understanding the optimization of this sampling process.

EXPERIMENTAL SECTION

Chemicals. The test mixture used throughout these experiments contains a series of poly(ethylene glycol) (PEG) and Brij surfactants. A 0.8% (w/w) stock solution of the PEG and Brij mixture contains an equal weight mixture of PEG 200, PEG 1000, PEG 8000, Brij 35, Brij 58, Brij 72, Brij 76, and Brij 78 in methanol. The test mixtures were further diluted (w/w) in methanol from the stock solution for the concentrations specified. The number following the PEG abbreviation is the number-average molecular weight and the number after the Brij name is a commercial designation. The exact molecular composition of the PEG and Brij surfactants is given in the caption to Figure 7. The PEG compounds were purchased from Polyscience (Warrington, PA), and the Brij surfactants were purchased from Aldrich Chemical Co. (Milwaukee, WI). All solvents (uninhibited tetrahydrofuran and methanol) were HPLC grade and purchased from J. T. Baker (Phillipsburg, NJ), except for the in-house water, which was purified by a Milli-Q system (Millipore Corp., Milford, MA).

Chromatographic Equipment. The reversed-phase HPLC column was a Zorbax SB18 (MAC-MOD Analytical, Chadds Ford, PA), 150 × 3.0 mm, with 5-μm particles and 80-Å pores. The styrene/divinylbenzene GPC column was from Polymer Standard Service (Mainz, Germany), 50 × 8.0 mm, with 3-μm particles and 100-Å pores. Short columns with small particle size are used so that relatively rapid elution can be accomplished in the second dimension (typically 40 s). This allows the 2DLC experiment to be run in the same amount of time as a one-dimensional HPLC experiment which takes ≈30 min.

Prior to the 2DLC experiments being run, one-dimensional experiments were carried out. The one-dimensional RPLC and

(14) Liu, Y.; Sweedler, J. V. *Anal. Chem.* **1996**, *68*, 3928−3933.
(15) Rezanka, T. *J. Chromatogr., A* **1996**, *727*, 147−152.
(16) Celis, J. E.; Bravo, R. *Two-Dimensional Gel Electrophoresis of Proteins*; Academic Press: New York, 1984.
(17) Venkatramani, C. J.; Phillips, J. P. *J. Microcolumn Sep.* **1993**, *5*, 511−516.
(18) Glockner, G. *Gradient HPLC of Copolymers and Chromatographic Cross-Fractionation*; Springer-Verlag: Berlin, 1991.
(19) Kilz, P.; Kruger, R. P.; Much, H.; Schulz, G. *Chromatographic Characterization of Polymers: Hyphenated and Multidimensional Techniques*; Advances in Chemistry Series 247; American Chemical Society: Washington, DC, 1995; Chapter 17.
(20) Yau, W. W.; Kirkland, J. J.; Bly, D. D. *Modern Size-Exclusion Liquid Chromatography*; John Wiley & Sons: New York, 1979.

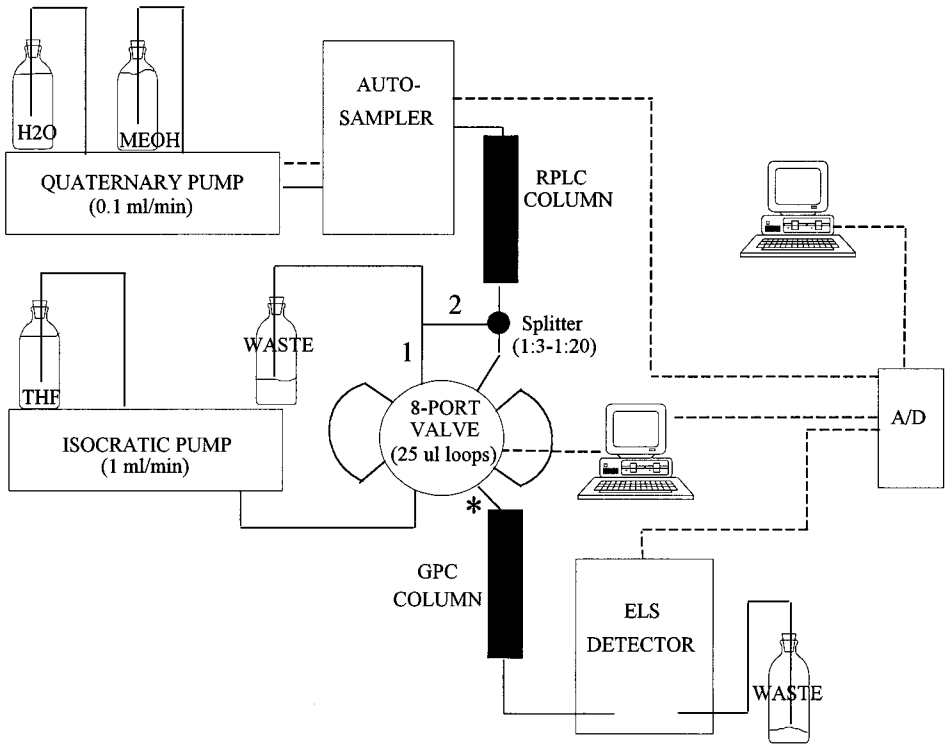

Figure 1. Schematic representation of the 2D HPLC instrument.

GPC experiments were conducted with a Perkin-Elmer (Norwalk, CT) model 410 pump, ISS-100 autosampler, and SEC-4 solvent chamber. The solvents were purged with helium for 15 min before pressurizing. The injection volume was 25 μL. The evaporative light scattering (ELS) detector (Sedex, model 55, Richard Scientific, Novato, CA) was set at 40 °C, 2.2 bar of house nitrogen, and a gain of 8.

The equipment used for the 2DLC experiments utilize RPLC as the first dimension and GPC as the second, configured as shown in Figure 1. The 2DLC system used the same equipment in the first dimension (RPLC) as the one-dimensional experiments, with the addition of a DuPont (Wilmington, DE) model 880 pump for the GPC apparatus, a Valco tee (Houston, TX) for splitting the first dimension effluent, and a Valco eight-port valve (model C8W with high-speed switching accessory and dual 25-μL loops) for collecting the first dimension effluent with subsequent injection into the second dimension.

First Dimension Flow Rate Adjustment. The splitting of the RPLC column effluent facilitates longer sample loop fill times and hence longer second dimension run times. The split ratio, S, between the RPLC and the eight-port valve was set by varying the ratio of lengths of fused-silica capillary (Polymicro Technologies, Phoenix, AZ) with 75-μm internal diameter between the two waste lines (labeled 1 and 2 in Figure 1). The length of the eight-port valve waste capillary (designated as 1 in Figure 1) was held constant at 90 cm. The waste line out of the tee (designated as 2 in Figure 1) was varied from 8 to 60 cm to increase the split ratio. The length was cut until the desired flow rate was measured out of the eight-port valve waste line.

Sampling Time. In comprehensive 2DLC systems, the sample loop volume, V_S, is related to the first dimension flow rate, F, and sampling time, t_S, as $V_S = Ft_S/S$. The sampling time is equal to the second dimension run time. Rearrangement of this equation for the sampling time gives $t_S = V_S S/F$. The run time in the second dimension is directly proportional to V_S and S and inversely proportional to F. The variation of V_S and F influence GPC resolution;[20] therefore, only S is varied to change t_S for the purpose of examining the two-dimensional resolution as a function of the number of second dimension samples across a first dimension peak. The parameters used in this paper, while keeping V_S (25 μL) and F (0.1 mL/min) constant, are shown in Table 2.

Table 2. Split Ratio, Sampling Time, Sample Concentration (C_S), and Amount Injected (q_2) onto the Second Dimension in the Sampling Time versus 2D Resolution Experiments

S	t_S (min)	C_S (%)	q_2 (μg)
3	0.67	0.15	1.25
4	1	0.20	1.25
6	1.5	0.30	1.25
8	2	0.40	1.25
12	3	0.60	1.25
16	4	0.80	1.25

Computer Interface. The valve was controlled with an AST (Irvine, CA) 386/16 computer with a National Instruments (Austin, TX) PC-TIO-10 timing and digital I/O board interfaced to the valve electronics. This system is run with a Visual Basic (Microsoft Corp., Redmond, WA) program. The hardware interface is shown in Figure 2. The interface uses two digital outputs from the I/O board, one to control the valve with quad NOR (Texas Instruments 7402) logic and the other to start the data acquisition system through a relay. The relay (Radio Shack 275-243) provides an isolated switch to trigger data acquisition. Alternatively, the data acquisition system can start the computer program by using a

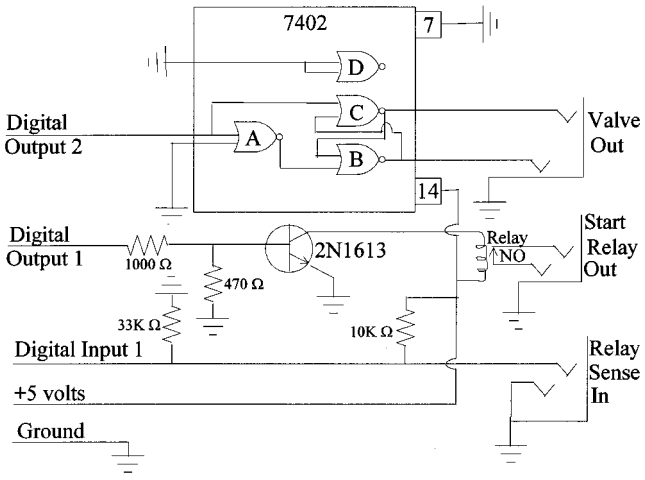

Figure 2. Schematic diagram of the interface between the National Instrument I/O board and the valve electronics. NO indicates normally open.

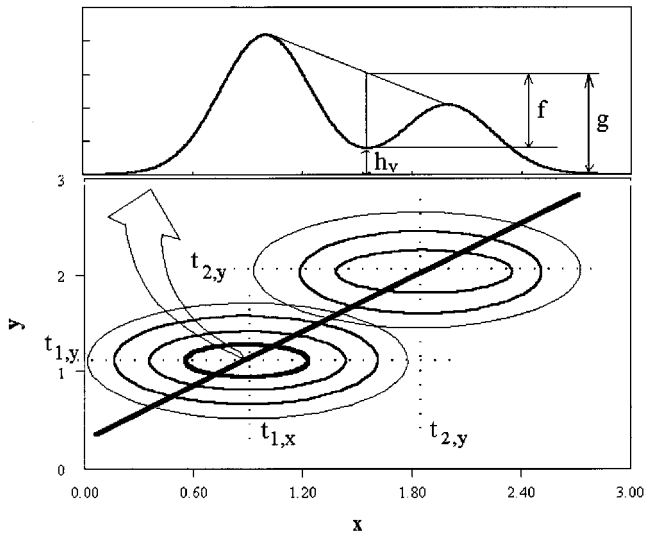

Figure 3. Schematic diagram of the two-dimensional resolution measurement using a 2D contour (bottom) and the corresponding slice for resolution determination.

relay connected via the relay sense input shown in Figure 2. In this mode of operation, the system can be used for repetitive autosampler-driven analysis. The transistor (Motorola 2N1613) is used to increase the output source current of digital output 1 to drive the relay. Stereo phone jacks and plugs are used to connect the computer interface to the high-speed valve switching electronics and the start and stop relays.

Data Processing. Data were collected from the ELS detector with a Turbochrom data acquisition system (PE Nelson, Cupertino, CA) using an acquisition rate of 5 Hz. The 2D data are collected as one Turbochrom file and processed with a FORTRAN program which produces an IEEE floating point format binary matrix file, and run on a Pentium-class PC. The matrix is read by Spyglass Transform (Fortner Research, Savoy, IL) and presented as a contour plot using a bilinear interpolation algorithm for 2D presentation and analysis. The peak and valley heights for the two-dimensional resolution measurements described below were read from the spreadsheet contained within Spyglass Transform. All experiments were run in triplicate for two-dimensional resolution measurements.

Measurement of Two-Dimensional Resolution. The multidimensional resolution, R_s, was recently suggested to be equal to the Euclidean norm of the resolution in each dimension.[21] Further research[22] showed that this definition, under a certain set of assumptions, could be utilized to produce an experimentally simple method for two-dimensional resolution estimation. We use and describe that method here.

The time between zone centers (δ) in each dimension is

$$\delta_x = (t_{2,x} - t_{1,x}) \qquad \delta_y = (t_{2,y} - t_{1,y}) \tag{1}$$

where $t_{1,x}$ and $t_{2,x}$ are the retention times of the peak maxima for peaks 1 and 2 in the x separation axis. The peak maxima in the y dimension are similarly denoted as $t_{1,y}$ and $t_{2,y}$. The corresponding two-dimensional resolution is defined as

$$R_S = \sqrt{R_{s_x}^2 + R_{s_y}^2} = \sqrt{\frac{\delta_x^2}{16\sigma_x^2} + \frac{\delta_y^2}{16\sigma_y^2}} \tag{2}$$

where σ_x and σ_y are the standard deviations of the zone in the x and y dimensions, respectively. It is noted that the standard deviations of peaks 1 and 2 are assumed to be equal in each dimension as required by this simple definition of two-dimensional resolution. R_{s_x} and R_{s_y} are the individual resolutions along the x and y coordinate axes.

Using eq 2, it is simple to derive[22] a method for determining R_s using the easy to measure peak to valley ratio, P, defined as f/g and shown in Figure 3. The peaks and valley in the contour plot of Figure 3 are hard to visualize; therefore, a line is overlaid on the contour chromatogram to show the resulting one-dimensional chromatogram at the contour peak maxima. The difference between the amplitude at the valley and average peak maximum is f, and the average peak maximum is g. The two-dimensional resolution is easily calculated[22] as

$$R_s = \sqrt{-\frac{1}{2}\ln\left(\frac{1-P}{2}\right)} \tag{3}$$

This method assumes that the peaks are Gaussian; this assumption has been checked with simulated tailing peaks and found to yield accurate resolution values for two-dimensional peaks when tailing is low to moderate.[23]

THEORY

In this section we will calculate the added contributions of zone broadening due to the finite volume sampling of the first dimension zone. This process can be viewed as a mixing or "deseparation" process whereby the eluting solute is stored and delivered to the second dimension separation system as an average concentration. We assume for this treatment that the volume of the sample loop is very much smaller than the second dimension

(21) Giddings, J. C. *Multidimensional Chromatography Techniques and Applications*; Chromatographic Science Series, 50; Marcel Dekker: New York, 1990; Chapter 1.
(22) Schure, M. R. *J. Microcolumn Sep.* **1997**, *9*, 169−176.
(23) Schure, M. R., manuscript in preparation.

column volume so that the injected volume of the sample is unimportant to the second dimension separation system. Furthermore, we assume that mixing in the sample loop is complete so that the temporal separation is lost within the loop. Although this assumption is not critical, it simplifies the theoretical development of zone broadening for this type of sample injection system. We will express this additional source of zone broadening in the first dimension due to finite volume sampling as σ_s.

The value of σ_s may be obtained through a series of steps. We first consider the average concentration of solute in the sample loop, $\bar{C}(t_{i-1}, t_i)$, which is obtained by

$$\bar{C}(t_{i-1}, t_i) = \frac{1}{t_s} \int_{t_{i-1}}^{t_i} C_1(t')\, dt' \tag{4}$$

where t' is the dummy variable of integration, $C_1(t')$ is the solute concentration profile from the column process in the first dimension, and t_{i-1} and t_i are the starting and stopping times, respectively, for solute collection in the sample valve. Note that $t_S = t_i - t_{i-1}$. For simplicity we further assume that C_1 is Gaussian so that

$$C_1(t) = \frac{1}{\sqrt{2\pi}\sigma} e^{-(t-\bar{t})^2/2\sigma^2} \tag{5}$$

where $\bar{t}$ is the temporal zone center and σ is the Gaussian standard deviation due to intracolumn processes.

The local average concentration, $\bar{C}(t_{i-1},t_i)$, can be expressed as a continuous time process, $C_S(t)$, for displaying the concentration profile of the sampled zone in the first dimension which is injected into the second dimension separation system:

$$C_S(t) = \sum_{i=1}^{N^+} [u(t - t_{i-1}) - u(t - t_i)] \bar{C}(t_{i-1},t_i) \tag{6}$$

In eq 6, $u(x)$ is the unit function such that $u(x) = 0$ when $x < 0$ and $u(x) = 1$ when $x \geq 0$. Furthermore, N is the number of samples across a Gaussian peak of baseline width 8σ so that $t_s = 8\sigma/N$. The terminology used in eq 6 is that $N^+ = N$ if $t_0 = \bar{t} - 4\sigma$, i.e., if the starting time for sample collection is exactly in phase with the peak arrival. If the sampling collection is out of phase with the peak arrival then $N^+ = N + 1$ because $t_0 < \bar{t} - 4\sigma$. In both cases, $t_i = t_{i-1} + t_S$. We do not need to consider the case of $t_0 > \bar{t} - 4\sigma$ due to symmetry of the Gaussian peak. We note that equating the baseline width of a Gaussian peak to 8σ is very conservative; smaller values such as 6σ could be used to approximate the baseline width. There is no exact value here because the Gaussian density function asymptotically approaches zero. If 6σ is used, 0.135% of the peak area is not included within these bounds. When 8σ is used as the baseline peak width 0.00317% of the peak area is not included. The results presented in the following sections are dependent on the choice of baseline width used; however, the differences are small and do not change the quantitative conclusions that are drawn from this work.

The concentration profile observed for the first temporal dimension when a two-dimensional separation is performed can be computed using eq 6. This is shown in Figure 4 for $N = 1$, 3, 10, and 30, along with the Gaussian peak which is used for the computation of these sampled concentration profiles. Notice that we assume that the sampling is exactly in phase with the peak arrival. Hence, the collection starts at the zone front where $t_0 = \bar{t} - 4\sigma$ and ends at $t_N = \bar{t} + 4\sigma$.

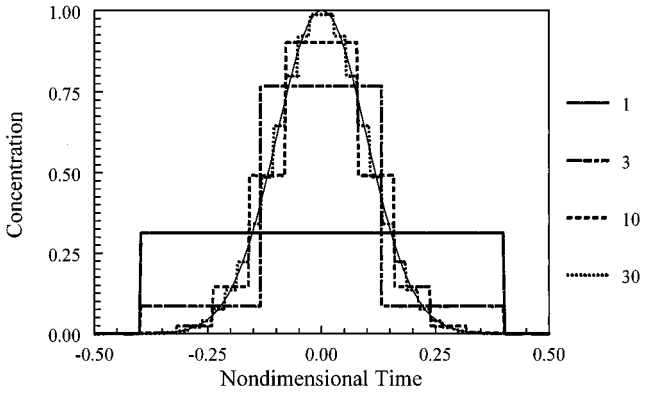

Figure 4. Concentration profiles for a Gaussian concentration density profile and the resulting in-phase "sampled" density profiles when $N = 1$, 3, 10, and 30. The time axis is nondimensional with $t = 10\sigma$ and with $\bar{t} = 0$.

The first dimension concentration profiles given in Figure 4 can be observed in the two-dimensional separation system when a detector is placed in the flow stream anywhere after the sampling valve (i.e., after the asterisk in Figure 1). In other words, these responses can be obtained even without a column in the second dimension and are simply a consequence of the finite volume injection measured in the first dimension.

As can be seen from Figure 4, the concentration profiles follow the original Gaussian concentration with the local average concentrations. Although not shown, the concentration profiles from the averaging process are identical for $N = 1$ and $N = 2$ due to symmetry. Although the averaging process appears to severely distort the peak shape at low N values, this is only a problem for accurate zone quantitation in the first separation dimension and does not affect the second dimension separation process nor second dimension zone quantitation.

The second central moment of any density function, $C(t)$, may be expressed as

$$M_2 = \int_{-\infty}^{+\infty} (t - \bar{t})^2 C(t)\, dt \tag{7}$$

when $C(t)$ is normalized so that $\int_{-\infty}^{+\infty} C(t) = 1$, as is the case with the Gaussian concentration density profile given in eq 5. We may now calculate the zone width as a function of the number of samples across the peak, N, which is obtained through the second moment by substituting $C_S(t)$ from eq 6 into $C(t)$ in eq 7 so that

$$M_2(N) = \int_{-\infty}^{+\infty} (t - \bar{t})^2 C_S(t)\, dt \tag{8}$$

Taking the square root of the second moment gives the standard deviation of the resulting series of rectangular profiles shown in Figure 4 as a function of N. Defining $\sigma_S = (M_2(N))^{1/2}$, the assessment of the increase in zone broadening due to sampling relative to the continuous peak width can be obtained by plotting

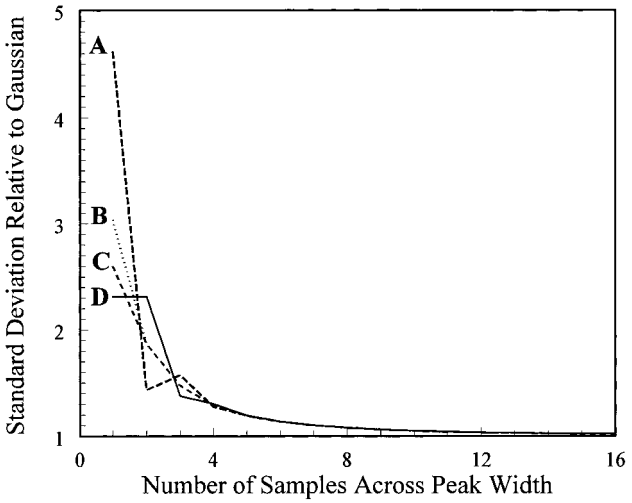

Figure 5. Quantity σ_S/σ as a function of N. (A) Sampling is $4\sigma/N$ prior to $t_0 = \bar{t} - 4\sigma$; (B) the average σ_S/σ; (C) sampling is $2\sigma/N$ prior to $t_0 = \bar{t} - 4\sigma$; (D) sampling is in phase (starts at $t_0 = \bar{t} - 4\sigma$).

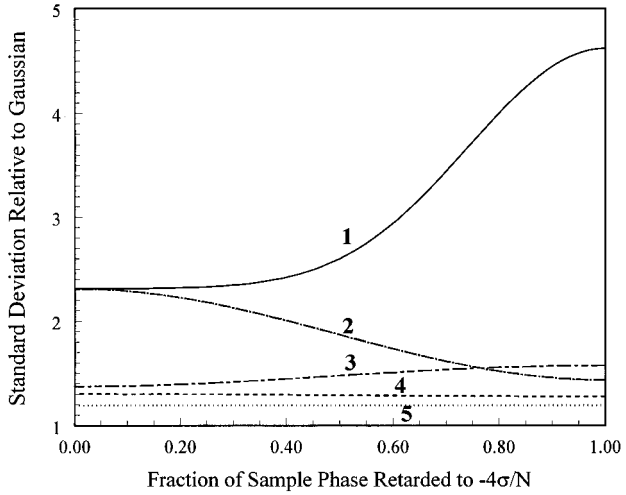

Figure 6. Quantity σ_S/σ for $N = 1$, 2, 3, 4, and 5 as a function of the fractional phase lag of $-4\sigma/N$ relative to t_0.

the nondimensional ratio σ_S/σ as a function of N, as given in Figure 5, for a number of cases which we discuss below. In all of these cases, we use numerically computed values as opposed to analytical solutions. Analytical solutions are possible for eq 8 but they are extremely complicated and offer no insight through inspection. The complexity requires the use of a computer to evaluate them. Hence, it is far easier and more flexible to calculate the integrals using Simpson's rule with very small grid sizes (for example 50 001 data points) and create the curves in this manner.

We have discussed the "in-phase" sampling case where sampling starts exactly at the beginning of the peak. In experimental practice, this cannot be guaranteed so that σ_S/σ must be investigated where the sampling phase is varied. As shown in Figure 5, σ_S/σ is plotted for four different cases, as explained in the figure caption. The average is computed by averaging 61 calculations of eq 8 where t_0 is varied from $t_0 = \bar{t} - 4\sigma - 4\sigma/N$ to $t_0 = \bar{t} - 4\sigma$.

A number of results come to light from Figure 5. First, all of these results converge to the same result at approximately $N \geq 4$. Hence, when four or more samples are taken across the peak width, it appears that the phase of the sampling process is unimportant. Second, the average σ_S/σ is monotonically decreasing with increasing N; however, two results shown here do not exhibit this monotonically decreasing response of the average. In the case of the in-phase result (curve D in Figure 5), σ_S/σ is equal for $N = 1$ and $N = 2$ because of the symmetry discussed above for $N = 1$ and $N = 2$ in Figure 4. The other case not showing a monotonically decreasing σ_S/σ is for curve A in Figure 5, where a local maximum occurs for $N = 3$; this curve is for the case where the sampling is maximally out of phase with the peak arrival. It is not obvious why a local maximum occurs for this special case, but this is further investigated below.

The quantity σ_S/σ is shown in Figure 6, as a function of the fractional phase delay for $N = 1$, 2, 3, 4, and 5. This helps explain some of the results from Figure 5. Here it is seen that t_0 will start at times smaller than $\bar{t} - 4\sigma$ (the in-phase start of sampling) by a fraction of $-4\sigma/N$ relative to t_0. When this fraction is zero, then sampling begins exactly at the in-phase start of sampling, and when the fraction is 1 in Figure 6, sampling is started at the maximally out-of-phase time. The effect is most pronounced for $N = 1$ and effectively vanishes for $N \geq 4$ although the effect is barely discernible at $N = 3$. The cases where $N = 1$, 2, and 3 are the most important cases since one wants to minimize N as much as possible to lift the restrictions of slow first dimension and fast second dimension run times.

The results for $N = 3$ in Figure 6 also show why the local maximum exists in Figure 5 for $N = 3$ at the largest out-of-phase condition. This is because the odd-numbered N results in Figure 6 increase with increasing sampling phase retardation while the even-numbered N curves decrease with increasing phase retardation. Hence, as shown in Figure 6, the results for $N = 2$ and $N = 3$ actually cross near the region of highest phase retardation leading to the result seen in Figure 5.

The results given in Figure 5 can be directly applied to the assessment of the total zone resolution. If the resolution in the first dimension is the dominant term to the total two-dimensional resolution, as given by the Euclidean norm (eq 2), then the total resolution will be reduced by a factor of σ/σ_S (the reciprocal of Figures 5 and 6) as a function of N. In this case, the mechanism of separation is predominately from the first dimension separation mechanism and the second dimension mechanism does not contribute toward zone resolution. For this scenario one might be better off simply utilizing one-dimensional chromatography with the first column and avoiding the mixing problems discussed in this paper. If the resolution in the first and second dimensions are roughly comparable, an increase in N will not proportionally affect the resolution, as dictated by eq 2, and the effect will be smaller than that shown in Figures 5 and 6. However, increasing the first dimension resolution by increasing N can also help increase the total resolution. For example, increasing the first dimension resolution by a factor of 2 will increase the total resolution by a factor of ~1.5 in this scenario. This may allow totally hidden peaks to become visible although fused, and fused peaks to become baseline-resolved. If the resolution in the second dimension is much larger than the resolution in the first dimension, the total resolution will be little affected by an increase in N. Hence, optimizing resolution as a function of N is pertinent

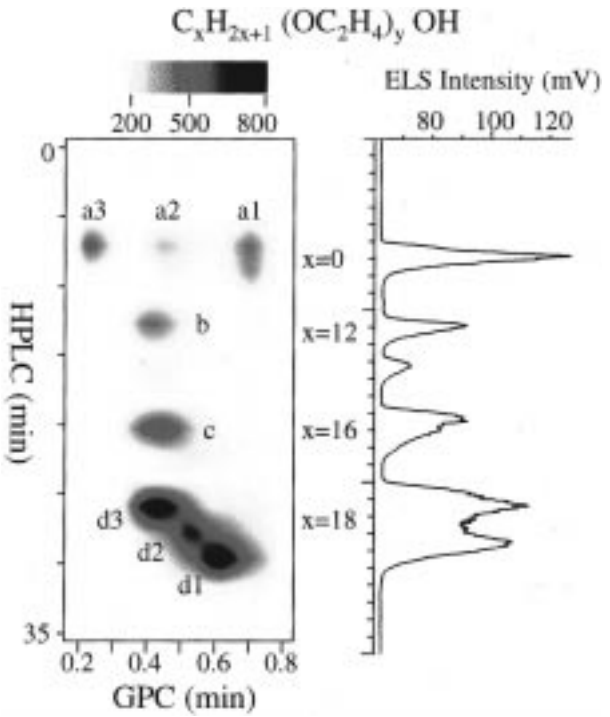

Figure 7. The 1D (right) and 2DLC (HPLC/GPC) (left) contour chromatogram of the PEG and Brij mixture. (a) PEG 200 (a1, $x = 0$, $y = 4.5$), PEG 1000 (a2, $x = 0$, $y = 23$), and PEG 8000 (a3, $x = 0$, $y = 182$); (b) Brij 35 ($x = 12$, $y = 23$); (c) Brij 58 ($x = 16$, $y = 20$); (d) Brij 72 (d1, $x = 18$, $y = 2$), Brij 76 (d2, $x = 18$, $y = 10$), and Brij 78 (d3, $x = 18$, $y = 20$). The HPLC flow rate is 0.1 mL/min and the solvent composition is 98/2 (methanol/water). The GPC flow rate is 1 mL/min tetrahydrofuran. The sampling time is 1.5 min and only 0.67 min of the GPC axis is shown.

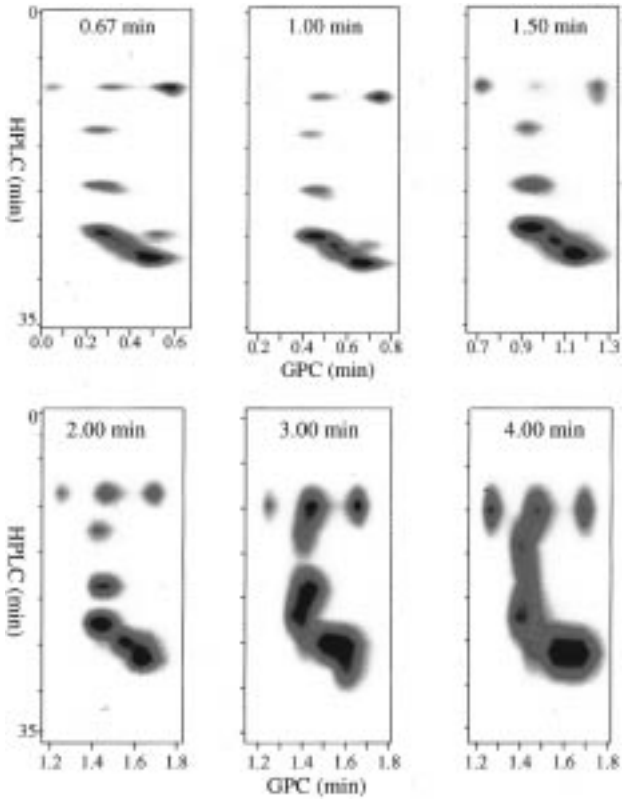

Figure 8. Sampling time effect on two-dimensional resolution, with conditions as in Figure 7. The sampling time is noted on each chromatogram, and 0.67 min of each GPC axis is shown for comparison purposes. Amplitude changes due to peak overlap cause a corresponding change in color between chromatograms.

when the first dimension separation is a strong contributor to the separation mechanism and to resolution.

RESULTS AND DISCUSSION

Effect of Sampling Time on Two-Dimensional Resolution. The 1D RPLC and 2D RPLC/GPC separation of the PEG and Brij mixture is shown in Figure 7. The one-dimensional RPLC experiment separates by alkyl chain length, *x*, where *x* is given in the formula listed in Figure 7. The selectivity for separation by the alkyl chain length is provided through some type of hydrophobic mechanism which is common for these types of molecules in RPLC. It is well-known that the ethylene oxide chain length, given as *y* in the formula listed in Figure 7, cannot be adequately separated by RPLC,[24] and in this regard the separation of the ethylene oxide subunits is accomplished by GPC. Thus, the 2DLC (RPLC/GPC) separation of these solutes takes place in the first dimension according to hydrophobicity (*x*) and in the second dimension according to the ethylene oxide chain length (*y*).

The separation is not totally orthogonal, as shown in Figure 7, and typical of most 2DLC (RPLC/GPC) separations.[19] Low molecular weight polymers, which can diffuse into the column pores, exhibit both hydrophobic and size retention mechanisms in reversed-phase HPLC and this mixed mechanism is shown by the Brij 70 series of peaks, d1−d3. The lower molecular weight material (d1) is more retained on the RPLC column since it can diffuse further into the pores.

(24) Rissler, K. *J. Chromatogr., A* **1996**, *742*, 1−54.

A series of experiments, outlined in Table 2, were carried out to monitor changes in two-dimensional resolution with sampling time into the second dimension. The sample concentration, C_S, injected into the first dimension was varied to keep the mass of solute injected into the second dimension constant. The relatively narrow range of sample concentrations did not affect resolution in the first dimension, as determined by preliminary experiments.

The results of these six 2DLC experiments are shown in Figure 8 where a decrease in R_s with an increase in the sampling time is seen to occur. The first three sampling times (0.67, 1.00, and 1.50 min) show a slight decrease in R_s with sampling time and peak broadening in the RPLC dimension. The second set of three times (2.00, 3.00, and 4.00 min) show a large loss in R_s with increased sampling time in the RPLC dimension with no apparent loss in the GPC dimension.

The measured two-dimensional resolution for each experiment is shown in Figure 9 in terms of the sampling time and the number of samples per first dimension peak width. Each dimension is represented by a pair of analytes; the resolution in the reversed-phase or *x* dimension is represented by the Brij 58/Brij 78 pair and the resolution in the GPC or *y* dimension is represented by the PEG 8000/PEG 1000 pair. The two-dimensional resolution of the PEG pair stays fairly constant because these analytes are exclusively separated by the second dimension, whereas the Brij pair decreases with an increase in sampling time.

The 8σ baseline peak width of the Brij 58 peak is 5.0 min in the first dimension. The highest resolution was attained at a 1.0-min sampling time or five samples across the peak ($N = 5$). For

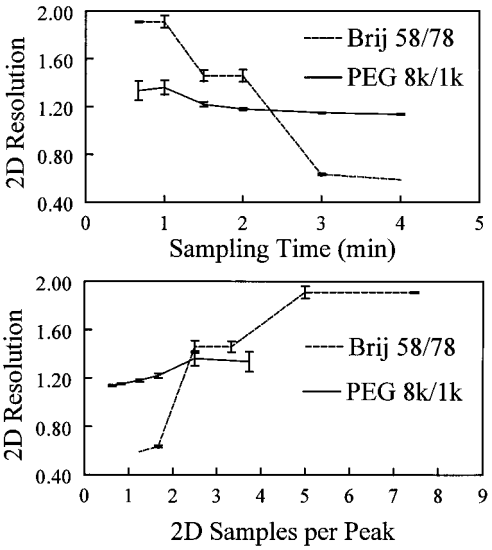

Figure 9. Effect of sampling time on two-dimensional resolution. The average and standard deviation of three replicate 2DLC runs are presented.

less than five samples across the peak, the resolution decreased substantially as shown in Figure 9. For the sampling time of 2.0 min ($N = 2.5$), the two-dimensional resolution of the Brij pair is ≈1.50, which yields baseline resolution. For larger sampling times (t_S of 3.0 and 4.0 min, $N = 1.67$ and 1.25), the Brij pair merges into one peak where all of the Brij components are unresolved. The reduction in the two-dimensional resolution of the Brij pair at longer sampling times ($N < 5$) is attributed to undersampling of the first dimension peak. Under these conditions, the peaks separated in the first dimension are recombined and the second dimension does not have the resolving power to separate them because of the predominately size-based separation mechanism in the second dimension. These experiments indicate that to preserve the resolution achieved in the first dimension, the number of samples should be ≈3 or greater across the peak width.

The results shown in Figure 9 are in substantial agreement with the theoretical results presented earlier. The increase in resolution when going from $N = 2.5$ to $N = 5$ is a factor of ~1.33. This compares very well with the ratio of the relative broadening from Figure 5, where a factor of ≈1.28 is noted to occur when going from $N = 2.5$ to $N = 5$.

Effect of Flow Rate on Two-Dimensional Resolution. The optimum flow rate of the first dimension column is approximately 0.3−0.5 mL/min as recommended by the manufacturer. In the sampling time versus two-dimensional resolution experiments, the first dimension flow rate was 0.1 mL/min, which results in a higher number of samples across the peak. A series of experiments were carried out with different first dimension flow rates to determine the effect of the number of samples per peak on two-dimensional resolution while keeping the sampling time constant.

The split ratio was varied in these experiments to facilitate a constant sampling time of 1.00 min and sample loop volume of 25 μL when the flow rate was varied. The split ratios, sample concentrations, and flow rates used in these experiments are listed in the caption to Figure 10. Note that the sample concentration was varied to keep the injection solute mass constant in the GPC column throughout these experiments.

The 2DLC results are shown in Figure 10. In these experiments the 8σ baseline peak widths of the Brij 58 peak in the first dimension are 5.0, 1.3, and 1.0 min for flow rates of 0.10, 0.30, and 0.50 mL/min, respectively. There is a reduced number of second dimension runs across the first dimension peak widths at higher flow rates. This results in a similar loss of resolution as in the sampling time experiments and is attributed to an undersampling of the first dimension. Thus, the zone velocity in the first dimension must be reduced to acquire enough second dimension samples to maintain high resolution.

The data from the sampling time and flow rate study are shown in Figure 11. The two studies show similar results for each solute pair. The PEG pair shows a slight decrease in two-dimensional resolution at $N < 2.5$. The Brij solute pair shows a dramatic decrease in two-dimensional resolution at $N < 5$. There was no measurable increase in R_s at $N \geq 5$. These results show that two-dimensional resolution is not affected by the sampling time for solutes whose separation mechanism acts in the second dimension. However, the two-dimensional resolution is strongly affected by sampling time for a RPLC/GPC 2DLC system when the effective separation mechanism acts in the first dimension.

The experimental data show that five samples ($N = 5$) are needed per first dimension peak to obtain high two-dimensional resolution. These results correlate well with Figure 5, where there is low peak broadening due to sampling at $N > 5$. At less than five samples per peak, there is increased broadening and a noticeable loss of resolution.

Effect of Sampling Phase on Two-Dimensional Resolution. The effect of sampling phase was studied at two different sampling times where the first dimension was sampled at approximately 2 and 4 times across the 8σ peak width while all other variables except sample concentration were kept constant. The sample concentrations are listed in Table 2 for the sampling times of 2 min ($N = 1.9$) and 1 min ($N = 3.8$).

The effect of sampling phase on resolution is shown in Figure 12. The sampling phase is experimentally varied by changing the start of the second dimension sampling through a delay time implemented in software. These results show that at approximately four samples taken across the first dimension peak width there is little if any effect on sampling phase. However, for the experiments where approximately two samples are taken across the first dimension peak width the results, shown on the bottom of Figure 12, indicate that there is a very large effect on sampling phase. These results show that the four two-dimensional chromatograms not only possess different resolutions between peaks but, in addition, differ visually because the large phase sensitivity is driven by a critical undersampling of the first dimension separation system. In this regard, the phase sensitivity when present is a nuisance in method development because it gives different results depending on the sampling process timing.

CONCLUSIONS

We have illustrated both experimentally and theoretically the result of systematic changes in sampling time and its effect on resolution. The results show that the shortest sampling time into the second dimension gives the best resolution and longer sampling times decrease resolution along the first dimension axis. The resolution in the second dimension was not affected by

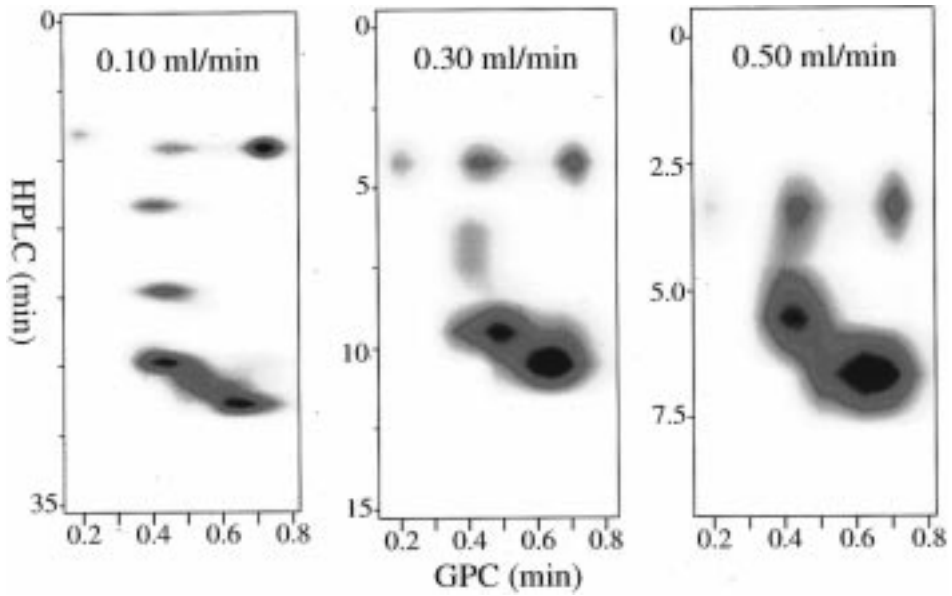

Figure 10. Effect of flow rate on two-dimensional resolution. The sampling time is 1 min. The split ratios are 4, 12, and 20 and sample concentrations 0.20, 0.60, and 0.80% for RPLC flow rates of 0.10, 0.30, and 0.50 mL/min, respectively. Other conditions as in Figure 7.

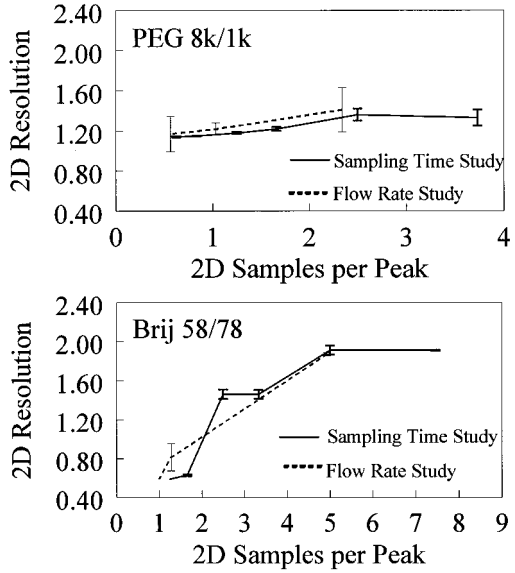

Figure 11. Number of second dimension samples per first dimension peak width effect on two-dimensional resolution. The average and standard deviation of three replicate 2DLC runs are presented.

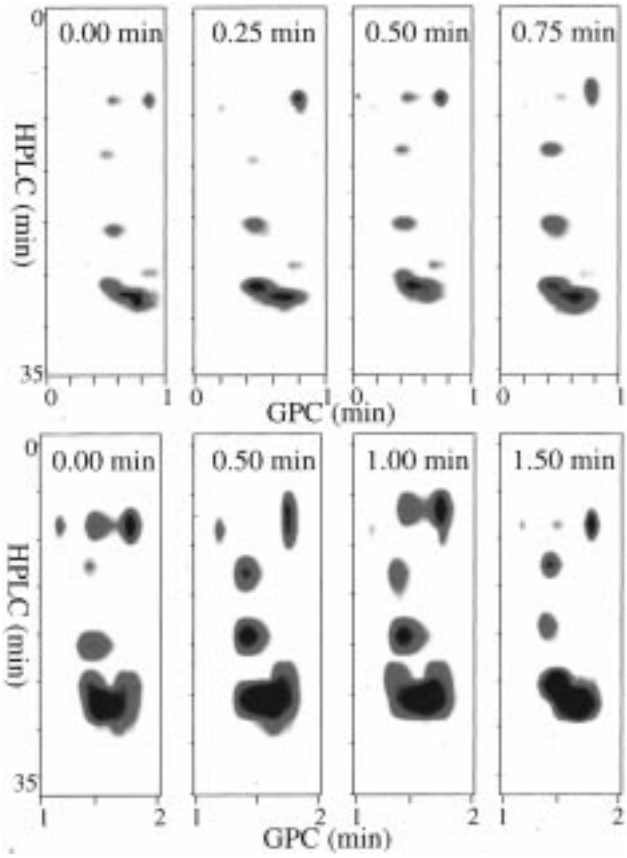

Figure 12. Sampling phase effect on two-dimensional resolution for N = 3.8 (top 4) and N = 1.9 (bottom 4). A sampling time of 1 min was used for the N = 3.8 study, and a sampling time of 2.0 min was used for the N = 1.9 study. The sampling phase is expressed as a delay time and noted on each chromatogram.

undersampling of the first dimension, but the overall result was a loss in two-dimensional resolution. To obtain the highest two-dimensional resolution, each separated peak in the first dimension should be sampled at least three times into the second dimension when the sampling is in-phase, whereas if the sampling phase is not considered, there should be at least four samples per peak.

These results can be used for decreasing the time for 2DLC method development. The second dimension method should be developed first to provide the fastest analysis time with adequate resolution. Then the first dimension should be operated to give an 8σ peak width of 4 times the second dimension elution window. If the first dimension peak width varies as a function of elution time, then the sampling time can also be varied as a function of elution time or the narrowest peak of interest in the first dimension can be used to establish the sampling rate. This method development scheme will result in the highest resolution in the shortest amount of time. As with any chromatographic system,

the 2DLC can be operated with a lower number of samples per peak ($N < 4$), to give a faster analysis time, but with a reduced resolution.

Polymers have an inherit polydispersity due to the many distributions present. The separation of polymers by composition and size distinguishes two of these distributions, and 2DLC offers the analyst a higher resolution and higher selectivity alternative to the one-dimensional LC techniques. We hope that the guidelines offered in this paper enhance the applicability of 2DLC and make it more widely used.

Received for review October 24, 1997. Accepted January 23, 1998.

AC971184B